



ISSN 2314-5609
Nuclear Sciences Scientific Journal
vol. 4, p 37 - 45
2015

NATURAL RADIOACTIVITY MEASUREMENTS IN LOCAL AND IMPORTED COMMERCIAL GRANITES USED AS ORNAMENTAL STONES

ABDEL MOEZ A. SADEK ; ABDEL HADI A. ABBAS and ANAS M. EL-SHERIF

Nuclear Materials Authority

ABSTRACT

^{238}U , ^{232}Th , ^{226}Ra , and ^{40}K radioactivities were determined in commercial granite samples collected from local market using a NaI (Tl) gamma-ray spectroscopy system. ^{238}U , ^{232}Th , ^{226}Ra , and ^{40}K activity concentrations of the studied commercial granites range between 31 and 351.33 BqKg^{-1} , 22.2 to 102.35 BqKg^{-1} , 22.2 to 168.35 BqKg^{-1} and 881.49 to 1460.67 BqKg^{-1} , respectively. The highest values of activity concentrations of ^{238}U , ^{226}Ra and ^{40}K were recorded in Lahm Mafroum commercial granites. High radioactivity of Lahm Mafroum is attributed to the presence of meta-autonite, zircon, allanite, monazite, sphene and apatite.

Absorbed Dose Rate (D), annual effective dose equivalent (AEDE), radium equivalent activity (Raeq), external (Hex) and internal (Hin) hazard index, in addition to activity gamma index (I γ) caused by gamma emitting natural radionuclide are determined from the obtained values of ^{226}Ra , ^{232}Th and ^{40}K . Fairly, many of the studied commercial granites do not satisfy the universal standards.

INTRODUCTION

Usually granites have a commercial name, petrographic and technological characterizations, and identification of the producer country (Abirochas, 2003; Pivko, 2003; Anjos et al., 2005). Granites, usually suitable as building and ornamental materials for interior and exterior use, are hard natural stones that require harder tools to be cut, shaped and polished, compared with marble. Distinct types of commercial granites have different geological origins and mineralogical compositions and may be either magmatic or metamorphic rocks. Thorium, uranium and potassium concentrations of granitic rocks are intimately related to their mineral compositions and general petrologic features (Whitfield et al., 1959; Rogers and Ragland, 1961; Doventon and Prensky, 1992). Uranium and thorium

in igneous and metamorphic rocks are usually found in a few accessory minerals such as apatite, sphene and zircon. Other highly radioactive minerals, like monazite, allanite, uraninite, thorite and pyrochlore, are widespread in nature, but they are very minor constituents of rocks. Uranium tends to be highly mobile near the surface whereas thorium is relatively stable. Uranium is easily oxidized to a water-soluble form and can be readily leached from pegmatites and granites and re-deposited in sediments at large distances from the source rock. Thorium is much less soluble than uranium and potassium and does not move except by mechanical means such as wind and erosion processes. Both thorium and uranium contents tend to be high in felsic rocks and to increase with alkalinity or acidity, with their highest concentrations found in pegmatites. The potassium content of rocks also increases

with acidity. It is usually found in potash feldspars, such as microcline and orthoclase, or in micas, like muscovite and biotite. Rocks that are free of these minerals have very low K-activity. The petrologic features of granitic rocks associated with effects of weathering and metamorphism produce expressive alterations in the relationship between the natural radionuclides (Th, U, K, Th/U and Th/K).

The study of the concentrations and distributions of the natural radionuclides in rock and soil allows the understanding of the radiological implication of these elements due to the gamma ray exposure of the body and irradiation of lung tissue from inhalation of radon and its daughters. In particular, it is also important to assess the radiation hazards arising due to the use of rock and soil in the construction of dwellings. Therefore, it is important to measure the concentration of radionuclides in rocks used as building materials for assessing the radiological risks to human health and for the use and management of these rocks. Several authors have studied the natural radioactivity level of rocks from different places (Xinwei, 2004; Xinwei et al., 2006).

Most of the naturally occurring radionuclides exist in rocks and soils at concentrations that are not of concern to human health or the environment (Elles and Lee 2002). But there are areas with relatively high natural concentrations of U, Ra and Th due to their geological evolution. Natural and anthropogenic accelerated radionuclides mobilization also occurs in areas with high background concentrations (Barnett et al., 2000). U and Th are long-lived radionuclides with a suite of radioactive daughter products which can pose a human-health and ecological risk. Radiation of natural origin is responsible for most of the total radiation exposure to the general population. Quantification of background levels of radionuclides is necessary to evaluate the potential environmental risk, to determine the boundary of areas of high natural background

and to establish its cleanup level (Elles and Lee 2002; Taboada et al., 2006; El-Aassy et al., 2012).

SAMPLING AND EXPERIMENTAL TECHNIQUES

Thirty six commercial granite samples used as building materials were collected from local markets representing local and imported types. Different locations of the local samples were recorded on Fig.(1). They subjected to radiometric analysis using NaI (TI) gamma-ray spectrometers for determination of their radioelements concentration and activity.

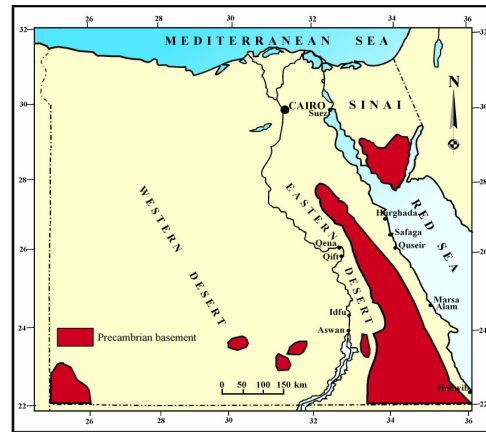


Fig. 1 : Different localities of commercial granite (El-Ramly, 1972)

These samples were prepared for gamma-ray spectrometric analysis in order to determine their uranium, thorium, radium and potassium contents by using multichannel analyzer of gamma-ray detector (Gamma-Spectrometer technique). The instrument used in determination of the four radioactive elements consists of a Bicorn scintillation detector NaI (TI) 76x76 mm, hermetically sealed with the photomultiplier tube in aluminum housing. The tube is protected by a copper cylinder protection of thickness 0.6 cm against induced X-ray and a chamber of lead bricks against environmental radiation. Uranium, thorium, radium and potassium are measured by using four energy regions

representing Th-234, Pb-212, Pb-214 and K-40 at 93 kV, 239 kV, 352 kV, and 1460 kV for uranium, thorium, radium and potassium, respectively. The measurements were carried out in sample plastic containers, cylindrical in shape, 212.6 cm³ volumes with 9.5 cm average diameter and 3 cm height. The rock sample is crushed to about 1 mm grain size, and then the container is filled with about 300-400 gm of the crushed sample sealed well and left for at least 21 days to accumulate free radon to attain radioactive equilibrium. The relation between the percentage of Rn-222 accumulation and time increase till reaching the steady stage after about 38 days (Matolin, 1991).

ASSESSMENT OF DOSE

Absorbed Dose Rate in Air (D)

The absorbed gamma dose rates in air at 1m above the ground surface for the uniform distribution of radionuclides (²²⁶Ra, ²³²Th and ⁴⁰K) were calculated by using Eq.(1) on the basis of guide lines provided by UNSCEAR (2000) (Fgün et al., 2007).

$$D \text{ (nGy/h)} = 0.462A_{Ra} + 0.604A_{Th} + 0.0417A_K \quad (1)$$

where A_{Ra} , A_{Th} and A_K are the average specific activities of ²²⁶Ra, ²³²Th and ⁴⁰K in Bq/kg, respectively.

Annual Effective Dose Equivalent (AEDE)

The annual effective dose equivalent (AEDE) was calculated from the absorbed dose by applying the dose conversion factor of 0.7 Sv/Gy and the outdoor occupancy factor of 0.2 (UNSCEAR, 2000, Fgün et al., 2007).

Radium Equivalent Activity (Ra_{eq})

The radium equivalent activity for the samples was calculated. The exposure to radiation (Tufail et al., 1992) can be defined in terms of the radium equivalent activity (Ra_{eq}), which can be expressed by the following equation:

$$Ra_{eq} = A_{Ra} + 10/7A_{Th} + 10/130A_K \quad (2)$$

where A_{Ra} , A_{Th} and A_K are the specific activities of Ra, Th and K, respectively, in Bq/kg.

External and Internal Hazard Index (H_{ex} and H_{in})

To limit the annual external gamma-ray dose (Saito and Jacob, 1995; Saito et al., 1998; UNSCEAR, 2000) to 1.5 Gy for the samples under investigation, the external hazard index (Hex) is given by the following equation:

$$H_{ex} = A_{Ra}/370 + A_{Th}/259 + A_K/4810 \quad (3)$$

The internal exposure to ²²²Rn and its radioactive progeny is controlled by the internal hazard index (H_{in}), which is given by Nada (2003):

$$H_{in} = A_{Ra}/185 + A_{Th}/259 + A_K/4810 \quad (4)$$

These indices must be less than unity in order to keep the radiation hazard insignificant (Lakehal et al., 2010; Baykara et al., 2010).

Activity Concentration Index (I_γ)

Another radiation hazard index called the representative level index, I_γ, is defined as follows (NEA-OECD, 1979):

$$I_{\gamma} = A_{Ra}/150 + A_{Th}/100 + A_K/1500 \quad (5)$$

where A_{Ra} , A_{Th} and A_K are the activity concentrations of ²²⁶Ra, ²³²Th and ⁴⁰K, respectively in Bq/kg (Abbady et al., 2005). The safety value for this index is ≤ 1 (El Galy et al., 2008; El-Aassy et al., 2012).

RESULTS AND DISCUSSION

Most of the studied commercial granite facies (coarse-, and fine-grained granites) have the same mineralogy (quartz, plagioclase, K-feldspar, biotite and muscovite) and only differ in their modal proportions. In the fine-grained facies the amounts of biotite are less than in the coarse-grained facies and muscovite more than biotite. The main difference between facies is textural: the coarse-grained granite can be either porphyritic or equigranular; fine-grained facies always have an equigranular texture and finer grain size. Petrographically, most of the the studied granites are alkali feldspar granites. They are medium-, to coarse-grained and consist essentially of perthites, quartz, oligoclase, microcline and biotite. They are normally of hypidiomorphic

granular texture. Perthites form euhedral microcline and orthoclase perthite crystals. The microcline perthites may dominate strongly over orthoclase perthites. The perthites include string, flame and feather types. Quartz occurs as anhedral grains, interstitial to the perthites. A graphic texture has been observed in few samples. Oligoclases are less abundant than perthites. It occurs as small interstitial crystals between quartz and perthites. Biotite occurs as brown to reddish green subhedral flaky crystals in minor amounts. The flakes are pleochroic and mottled with iron oxides.

Uranium Bearing Minerals

Accessory minerals are represented mainly by zircon, allanite, monazite, sphene, apatite and fluorite. Zircon occurs as small subhedral to euhedral crystals. It is also observed as inclusions in quartz, biotite and chlorite. Some zircon crystals are occasionally metamict and surrounded by strong pleochloric haloes due to radiogenic effects (Fig.2). It is sometimes zoned, often associated and rimmed by iron oxides (Fig.3). Allanite occurs as few subhedral to euhedral reddish brown medium-grain size crystals intimately associated with biotite (Fig.4). Monazite occurs as small euhedral to subhedral, prismatic crystals enclosed within biotite and quartz (Fig.5). Their colours vary from pale yellow to yellowish brown. Sphene is found as euhedral sphenoidal shaped characterized by perfect cleavage, usually associated with mafic minerals (Fig.6). Fluorite occurs as colorless or violet anhedral grains. Opaques are disseminated as fine-grained within the mica or feldspar plates.

Secondary Uranium Minerals

In the oxidation zone, U^{+4} is oxidized to uranyl ion U^{+6} which is soluble and mobile in solutions and easy to combine with other cations such as Ca^{+2} , Cu^{+2} and Pb^{+2} , and anions such as those present in the form of sulphates and phosphates tend to form secondary uranium minerals such as uranophane, beta-uranophane, kasolite, torbernite, autunite and

meta-autunite. Autunite & Meta-autunite $[Ca(UO_2)_2(PO_4)_2 \cdot 2-6H_2O]$ represents the secondary uranium minerals in highly radioactive type of the studied commercial granites (Lahm Mafrum). The aggregates of autunite and meta-autunite are soft and consist of lemon yellow to

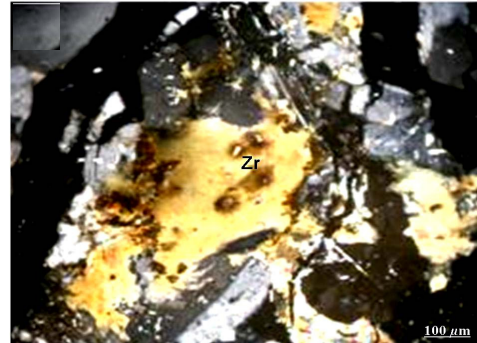


Fig.2: Pleochroic haloes around zircon crystals (Zr) in biotite, XPL

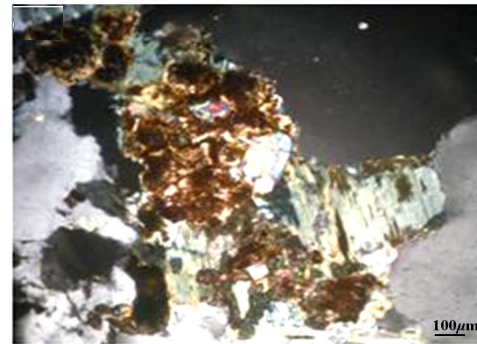


Fig.3: Iron oxides surrounded zoned zircon in chlorite, XPL

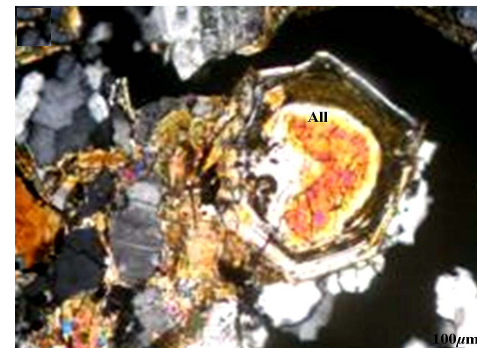


Fig.4: Zoned allanite crystal(All) , XPL

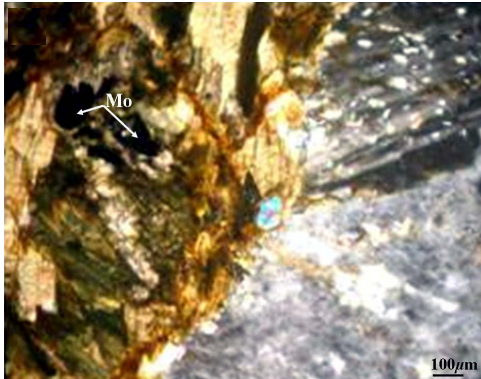


Fig.5 :Monazite crystal (Mo) in biotite, XPL



Fig.6: Sphene (Tit) and apatite (Ap) in quartz, XPL

greenish yellow small crystallites with a micaceous habit. Occasionally meta-autonite is found as tabular square crystals often in parallel growths and terminated by bipyramidal forms. This mineral contains 11.87% P_2O_5 , 46.80% UO_2 and the associated minerals contain 2.81% K_2O , 31.14% CaO , 0.42% MnO , 1.90% Fe_2O_3 , 2.98% SiO_2 , 1.59 % SO_3 and 0.48% Al_2O_3 , as detected by ESEM (Fig.7). The presence of meta-autonite crystals were confirmed by XRD technique (Fig.8).

Environmental Impacts

The average activity concentrations for granite are shown in Table (1), in which ^{238}U , ^{226}Ra , ^{40}K and ^{232}Th were 351.33 $Bqkg^{-1}$, 168.35 $Bqkg^{-1}$, 1460.67 $Bqkg^{-1}$ for (Lahm Ma-

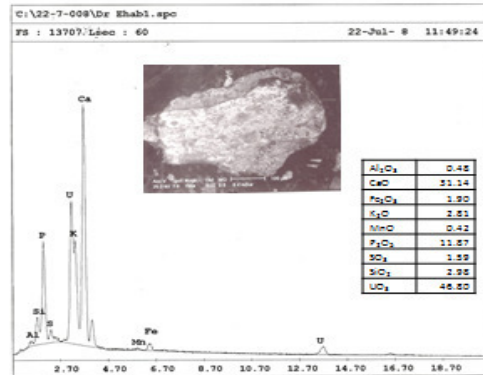


Fig.7: SEM backscattered image and EDX analyses for the separated meta-autonite

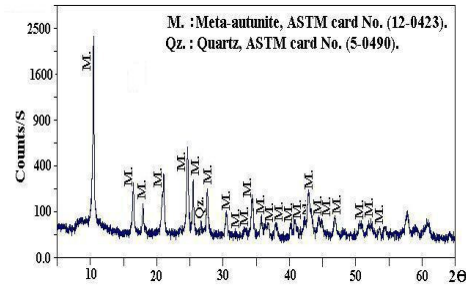


Fig. 8 : XRD pattern of the studied meta-autonite

froum) and 102.35 $Bqkg^{-1}$ for (Abradour), respectively. Minimum average activity concentrations of ^{238}U , ^{232}Th , ^{226}Ra and ^{40}K were 31.00 $Bq kg^{-1}$ for (Rosa Nasr), 22.22 $Bqkg^{-1}$ for (Fard Ghazal), 22.20 $Bqkg^{-1}$ for (Rosa Nasr) and 881.49 $Bqkg^{-1}$ for (Ramady), respectively. Average activity concentrations of the studied commercial granites were lower than activity concentration of commercial Chinese acidic granite (Xinwei et al., 2006) (Table 1). The lowest activity concentrations were recorded in Rosa Nasr and Ramady where the highest values were in Lahm Mafroum, Ahmer Aswan and Al Shaieb. High radioactivity of Lahm Mafroum is attributed to the presence of meta-autonite, zircon, allanite, monazite, sphene and apatite (Figs.2-6).

The average absorbed γ dose rate (D) values for commercial granite samples are shown

in Table (1). The values obtained in all the studied samples ranged between 81.50 and 262.27 nGyh⁻¹ with an average 154.00 nGyh⁻¹. These estimated values of absorbed γ dose rate in the studied samples are comparably higher than the world average value 57 nGyh⁻¹ (Tzortzis et al., 2003, Abbady et al., 2005).

Furthermore, the average values of annual effective dose for all commercial granite samples were also listed. The values obtained varied between 0.10 and 0.32 mSvy⁻¹. The mean value (0.19) found to be less than 0.48 mSvy⁻¹ [recommended by UNSCEAR, 2000] as the worldwide average of the annual effective dose.

Table 1 : Results of radionuclide concentrations, the dose rate (D), the annual effective dose equivalent (AEDE), radium equivalent activity (Ra_{eq}), external (H_{ex}), internal (H_{in}) hazard indices and gamma index (I_γ) for samples.

S.No.	Location	Commercial Name	eU BqKg ⁻¹	eTh BqKg ⁻¹	Ra BqKg ⁻¹	K BqKg ⁻¹	D (nGy/h)	AEDE (mSv/y)	Ra _{eq} BqKg ⁻¹	H _{ex}	H _{in}	I _γ
1	Aswan	Ahmer Aswan.1	74.4	56.56	33.3	1399.11	126.88	0.16	221.72	0.71	0.91	1.99
2		Ahmer Aswan.2	421.6	84.84	344.1	1205.05	296.27	0.36	558.00	1.72	2.86	4.46
3		Ahmer Aswan.3	62	56.56	44.4	1424.15	122.19	0.15	234.75	0.68	0.85	1.93
4		Ahmer Aswan.4	62	48.48	44.4	1361.55	114.70	0.14	218.39	0.64	0.81	1.81
5		Ahmer Aswan.5	161.2	68.68	66.6	1283.3	169.47	0.21	263.43	0.97	1.40	2.62
6		Ahmer Aswan.6	124	68.68	44.4	1314.6	153.59	0.19	243.64	0.87	1.21	2.39
Av.	Ahmer Aswan	150.87	63.97	96.20	1331.29	163.85	0.20	289.99	0.93	1.34	2.53	
7	South Sinai	Ramady.1	86.8	44.44	44.4	1054.81	110.93	0.14	189.02	0.63	0.86	1.73
8		Ramady.2	74.4	56.56	55.5	948.39	108.08	0.13	209.25	0.62	0.82	1.69
9		Ramady.3	99.2	36.36	99.9	867.01	103.95	0.13	218.54	0.59	0.86	1.60
10		Ramady.4	148.8	36.36	77.7	795.02	123.86	0.15	190.80	0.71	1.11	1.89
11		Ramady.5	173.6	44.44	66.6	1007.86	149.07	0.18	207.61	0.85	1.32	2.27
12		Ramady.6	148.8	40.4	66.6	838.84	128.13	0.16	188.84	0.73	1.13	1.96
13		Ramady.7	62	36.36	44.4	798.15	83.89	0.10	157.74	0.47	0.64	1.31
14		Ramady.8	74.4	40.4	33.3	741.81	89.71	0.11	148.08	0.51	0.71	1.39
Av.	Ramady	108.50	41.92	61.05	881.49	112.2025	0.1375	188.735	0.63875	0.93125	1.73	
15	South Sinai	Fard Ghazal.1	62	24.24	44.4	1183.14	92.62	0.11	170.04	0.51	0.67	1.44
16	Sharm El Sheikh	Fard Ghazal.2	272.8	12.12	99.9	1233.22	184.78	0.23	212.08	1.04	1.78	2.76
17		Fard Ghazal.3	24.8	32.32	44.4	1205.05	81.23	0.10	183.27	0.44	0.51	1.29
18		Fard Ghazal.4	86.8	24.24	22.2	1158.1	103.04	0.13	145.91	0.57	0.80	1.59
19		Fard Ghazal.5	86.8	12.12	33.3	1205.05	97.67	0.12	143.31	0.53	0.77	1.50
20		Fard Ghazal.6	24.8	28.28	22.2	1101.76	74.48	0.09	147.35	0.41	0.47	1.18
Av.		Fard Ghazal	93.00	22.22	44.40	1181.05	105.64	0.13	166.99	0.58	0.83	1.63
21	Hurgada	Lahm Mafrout.1	1066.4	48.48	543.9	1302.08	576.26	0.71	713.32	3.34	6.22	8.46
22		Lahm Mafrout.2	111.6	68.68	55.5	1461.71	154.00	0.19	266.05	0.87	1.17	2.41
23		Lahm Mafrout.3	74.4	64.64	55.5	1273.91	126.54	0.16	245.84	0.72	0.92	1.99
24		Lahm Mafrout.4	99.2	72.72	44.4	1474.23	151.23	0.19	261.69	0.86	1.12	2.37
25		Lahm Mafrout.5	111.6	64.64	55.5	1433.54	150.38	0.18	258.12	0.85	1.15	2.35
26		Lahm Mafrout.6	644.8	68.68	255.3	1818.53	415.21	0.51	493.30	2.39	4.13	6.20
Av.	Lahm Mafrout	351.33	64.64	168.35	1460.67	262.27	0.32	373.05	1.51	2.45	3.96	
27	Hurgada	Al Shaieh.1	223.2	121.2	144.3	1161.23	224.75	0.28	406.77	1.31	1.92	3.47
28		Al Shaieh.2	62	40.4	33.3	951.52	92.72	0.11	164.21	0.52	0.69	1.45
29		Al Shaieh.3	173.6	117.16	122.1	1314.6	205.79	0.25	390.59	1.19	1.66	3.21
Av.		Al Shaieh	152.93	92.92	99.90	1142.45	174.42	0.21	320.52	1.01	1.42	2.71
30	Imported	Abraadour.1	124	117.16	77.7	1527.44	191.75	0.24	362.57	1.11	1.44	3.02
31	Italian and	Abraadour.2	86.8	109.08	99.9	1395.98	164.20	0.20	363.11	0.95	1.18	2.60
32	Brazilian	Abraadour.3	111.6	80.8	55.5	1389.72	158.31	0.19	277.83	0.90	1.20	2.48
Av.	granites	Abraadour	107.47	102.35	77.70	1437.71	171.42	0.21	334.50	0.99	1.27	2.70
33	Aswan	Gandoula.1	111.6	92.92	55.5	1273.91	160.80	0.20	286.24	0.93	1.23	2.52
34		Gandoula.2	124	76.76	66.6	1364.68	160.56	0.20	281.23	0.92	1.25	2.50
Av.	Gandoula	117.80	84.84	61.05	1319.30	160.68	0.20	283.74	0.93	1.24	2.51	
35	El Ain El	Rosa Nasr.1	37.2	28.28	22.2	1245.74	86.21	0.11	158.43	0.47	0.57	1.36
36	Sukhna	Rosa Nasr.2	24.8	32.32	22.2	1098.63	76.79	0.09	152.88	0.42	0.49	1.22
Av.	Rosa Nasr	31.00	30.30	22.20	1172.19	81.50	0.10	155.66	0.45	0.53	1.29	
International average			-	45	32	420	57	0.48	370	1	1	0.5
Chinese acidic granite (Xinwei et al., 2006)			-	79.6	99.9	1128	57	0.48	370	1	1	0.5

Values of eU, eTh and eRa in ppm, as well as K, in %, were converted to activity concentration, Bq kg⁻¹, using the conversion factors given by Polish Central Laboratory for Radiological Protection (Malczewski et al., 2004; Said et al., 2010)

The radium equivalent activity Ra_{eq} for Egyptian and imported commercial granites ranges between 155.66 and 373.05 $Bq\ Kg^{-1}$ with 264.15 $Bq\ Kg^{-1}$ as a mean value. These values are lower than the recommended maximum value of 370 $Bq\ kg^{-1}$, with the exception of Lahm Mafroum Ra_{eq} is significantly higher than the maximum permitted value.

The values of external and internal hazard indices (H_{ex} and H_{in}) for the studied commercial granites range between 0.45 and 1.51 and 0.53 to 2.45, respectively. External and internal hazard indices are higher than unity for most studied granites indicating that these granites can not be used as building and interior decorative material of dwelling.

The gamma activity index ($I\gamma$) used to assess safety requirement for building materials were evaluated and presented in Table (1). The obtained values for both of them ranged between 1.29 and 3.96 with 2.38 as an average. The obtained values of gamma activity indices in all commercial granite samples were higher dose criterion ($0.3mSv\ y^{-1}$) and corresponds to an activity concentration index of $2 \leq I\gamma \leq 6$ proposed by EC (1999) for materials used in bulk construction.

Contribution of ^{238}U , ^{232}Th and ^{40}K radionuclides for the absorbed dose rate within the studied rocks are plotted on Fig. (9). It is clear that the contribution of ^{238}U , ^{232}Th and ^{40}K are different for most rock varieties. ^{40}K plays the main and most important role in dose rate contribution.

CONCLUSIONS

Maximum activity concentrations of ^{238}U , ^{226}Ra , ^{40}K and ^{232}Th were 351.33 $Bqkg^{-1}$, 168.35 $Bqkg^{-1}$, 1460.67 $Bqkg^{-1}$ for (Lahm Mafroum) and 102.35 $Bqkg^{-1}$ for (Abradour), respectively. Minimum concentrations of ^{238}U , ^{232}Th , ^{226}Ra and ^{40}K were 31.00 $Bqkg^{-1}$ for (Rosa Nasr), 22.22 $Bqkg^{-1}$ for (Fard Ghazal), 22.20 $Bqkg^{-1}$ for (Rosa Nasr) and 881.49 $Bqkg^{-1}$ for (Ramady), respectively. The highest values of activity concentrations of ^{238}U , ^{226}Ra and ^{40}K were recorded in Lahm Mafroum commercial granites. High radioactivity of Lahm Mafroum is attributed to the presence of meta-autonite, zircon, allanite, monazite, sphene and apatite.

Absorbed Dose Rate (D), annual effective dose equivalent (AEDE), radium equivalent activity (Ra_{eq}), external (H_{ex}) and internal (H_{in}) hazard index in addition to activity

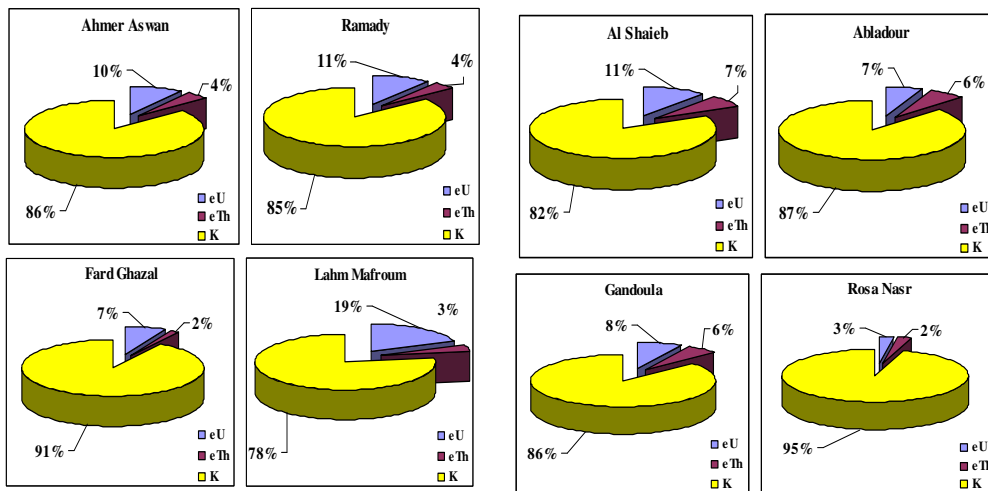


Fig. 9 : Contribution of ^{238}U , ^{232}Th and ^{40}K radionuclides for the absorbed dose rate within the studied rock samples

gamma index (I_γ) caused by gamma emitting natural radionuclide are determined from the obtained values of ^{226}Ra , ^{232}Th and ^{40}K . Fairly, many of the studied commercial granites do not satisfy the universal standards.

REFERENCES

- Abbadly, A.G.E.; Uosif, M.A.M. and El-Taher, A., 2005. Natural radioactivity and dose assessment for phosphate rocks from Wadi El-Mashash and El-Mahamid Mines, Egypt. *J. Environ. Radioact.*, 84, 65–78.
- Abirochas, 2003. Brazilian Dimension Stones Catalogue. Associação Brasileira de Indústria de Rochas Ornamentais-ABIROCHAS. <http://www.abirochas.com.br>.
- Anjos, R.; Veiga, R.; Soares, T.; Santos, A.; Aguiar, J.; Frascac, M.; Brage, J.; Uzeda, D.; Mangia, L.; Facure, A.; Mosquera, B.; Carvalho, C. and Gomes, P., 2005. Natural radionuclide distribution in Brazilian commercial granites. *Radiat. Meas.*, 39, 245–253.
- Baykara, O.; Karatepe, S. and Doğru, M., 2010. Assessments of natural radioactivity and radiological hazards in construction materials used in Elazığ, Turkey. Technical Report. *Radiat. Meas.* doi: 10.1016 / Jour. Radmeas. 2010.08.010. (In press).
- Barnett M.O.; Jardine P.M.; Brooks S.C. and Selim H.M., 2000. Adsorption and transport of uranium (VI) in subsurface media. *Soil Sci. Soc. Am. J.*, 64, 908–917
- Doventon, J.H. and Prenskey, S.E., 1992. Geological applications of wireline logs: a synopsis of developments and trends. *Log Anal.*, 33 (3), 286–303.
- El-Aassy I. E.; Afaf A. N.; El-Galy, M.M.; El-Feky M.G.; Abdel Maksoud, T.M.; Talaat, Sh.M. and Ibrahim, E.M., 2012. Behavior and environmental impacts of radionuclides during the hydrometallurgy of calcareous and argillaceous rocks, Southwestern Sinai, Egypt. *Appl. Rad. and Isotopes*, 70, 1024–1033.
- Elles, P. and Lee, S.Y., 2002. Radionuclide-contaminated soil: a mineralogical perspective for their remediation. In: *Soil mineralogy with environmental applications*, Chap. 25 (Dixon, J.B. & Schulze, D.G. Eds.). Soil Sci Soc. of America, Madison, 737–763
- El-Galy, M.M.; El-Mezayen, A.M.; Said, A.F.; El Mowafy, A.A. and Mohamed, M.S. 2008. Distribution and environmental impacts of some radionuclides in sedimentary rocks at Wadi Nasseib area, Southwest Sinai, Egypt. *J. Environ. Radioact.* 99, 1075–1082.
- El-Ramly, M.F., 1972. A new geological map for the basement rocks in the Eastern and South Western Deserts of Egypt, scale 1:1000,000. *Ann. Geol. Surv. Egy.*, II, 1-18.
- Lakehal, Ch.; Ramdhane, M. and Boucenna, A., 2010. Natural radionuclide concentrations in two phosphate ores of East Algeria. *J. Environ. Radioact.* 101, 377–379.
- Malczewski, D. and Taper, L., Dorda, J., 2004. Assessment of natural and anthropogenic radioactivity levels in rocks and soils in the environs of Swieradow Zdroj in Sudetes, Poland by in situ gamma-ray spectrometry. *J. Environ. Radioact.* 73, 233 – 245.
- Matolin, M., 1991. Construction and use of spectrometric calibration pads, Laboratory of gamma-ray spectrometry. A report to the government of the Arab Republic of Egypt, 4, 030-03.
- Nada, A., 2003. Evaluation of natural radionuclides at Um-Greifat area, Eastern Desert of Egypt. *Appl. Radiat. Isot.* 58, 275–280.
- Nuclear Energy Agency (NEA-OECD), 1979. Exposure to Radiation from Natural Radioactivity in Building Materials. Report by NEA Group of Experts. OECD, Paris.
- Öğün, Y.; Altınsoy, N. S.; Ahin, S.Y.; Güngör, Y.; Gültekin, A.H.; Karahan, G. and Karacık, Z., 2007. Natural and anthropogenic radionuclides in rocks and beach sands from Ezine region (Canakkale), Western Anatolia, Turkey. *Appl.*

- Radiat Isot, 65,739-747
- Pivko, D., 2003. The World's Most Popular Granites. <http://www.findstone.com>.
- Rogers, J.J.W. and Ragland, P.C., 1961. Variation of thorium and uranium in selected granitic rocks. *Geochim. Cosmochim. Acta*, 25, 99-109.
- Said, A.F.; Salam, A.M.; Hassan, S.F. and Mohamed, W.S., 2010. Assessment of the Environmental Radioactivity Impacts and Health Hazards Indices at Wadi Sahu Area, Sinai, Egypt. 10th Radiation Physics & Protection Conf., Nasr City, Cairo, Egypt.
- Taboada, T.; Cortizas, A.M.; Garcí'a, C. and Rodeja, E.G., 2006. Uranium and thorium in weathering and pedogenetic profiles developed on granitic rocks from NW Spain. *Sci Total Environ.*, 356, 192-206.
- Tufail, M.; Ahmad, N.; Mirza, S.M.; Mirza, N.M. and Khan, H.A., 1992. Regular paper, natural radioactivity from the building materials used in Islamabad and Rawalpindi, Pakistan. *Sci. Total Environ.*, 121, 283-291.
- Tzortzis, M.; Tsertos, H.; Christofides, S. and Christodoulides, G., 2003. Gamma-ray measurements of naturally occurring radioactive samples from Cyprus characteristic geological rocks. *Radiat. Meas.*, 37, 221-229.
- UNSCEAR, 2000. United Nations Scientific Committee on the effects of atomic radiation, sources and effects of ionizing radiation. Report to General Assembly, with Scientific Annexes United Nations. United Nations, New York.
- Whitfield, J.M.; Rogers, J.J.W. and Adams, J.A.S., 1959. The relationship between the petrology and the thorium and uranium contents of some granitic rocks. *Geochim. Cosmochim. Acta*, 17, 248-271.
- Xinwei, L., 2004. Natural Radioactivity in some building materials of Shaanxi, China. *J. Radioanal. Nucl. Chem.*, 262, 775-777.
- Xinwei, L.; Lingqing, W. and Xiaodan, J., 2006. Radiometric analysis of Chinese commercial granites. *Jour. Radioanal. Nucl. Chem.*, 267, 673-699.

القياسات الإشعاعية للجرانيت التجاري المحلي والمستورد والمستخدم كصخور للزينة

عبد المعز علي صادق، عبد الهادي أحمد عباس وأنس مالك الشريف

تم تحديد النشاط الإشعاعي الناتج من عناصر اليورانيوم²³⁸، الثوريوم²³²، الروديوم²²⁶ والپوتاسيوم⁴⁰ في عينات جرانيتية تجارية مجمعة من السوق المحلي باستخدام نظام تحليل أشعة جاما الطيفي. وقد تراوح تركيز هذه العناصر في الجرانيت التجاري من ٣١ إلى ٣٥١,٣٣ ومن ٢٢,٢ إلى ١٠٢,٣٥ ومن ٢٢,٢ إلى ١٦٨,٣٥ ومن ٨٨١,٤٩ إلى ١٤٦٠,٦٧ بيكريل/كيلوجرام للعناصر الأربعة على الترتيب. إن أعلى قيمة لتركيز النشاط الإشعاعي للعناصر الأربعة تم تسجيلها في الجرانيت التجاري المسمى (لحم مفروم) وهو يعود إلى إحتواءه على معادن الميتا-اوتونايت، الزركون، الألائيت، المونازيت، السفين والأباتيت. وبدراسة العوامل المؤثرة على البيئة المحيطة وجد أن معظم هذه العوامل أعلى من المعدلات العالمية، لذا فينصح بالحذر عند استخدام بعض هذه الأنواع من الجرانيت التجاري.